AIAA SciTech
4-8 January 2016, San Diego, California, USA
AIAA Guidance, Navigation, and Control Conference

Online Pilot Model Parameter Estimation Using Sub-Scale Aircraft Flight Data

Tanmay K. Mandal* and Yu Gu†
West Virginia University, Morgantown, WV, 26505, USA

Human pilots exhibit a wide range of control behavior changes even during the same phase of the flight. In this paper, an Unscented Kalman Filter (UKF) based real-time pilot model parameter identification algorithm is presented for longitudinal control of an aircraft. The UKF estimates the parameters of a lead-lag pilot model using pilot inputs and flight data collected using a Sub-Scale Research Aircraft (SSRA). The study is focused on the approach and landing phase of the flight. The real time estimation of the parameters can help identify changes in pilot control behavior that could lead to Loss of Control (LOC) events.

Nomenclature

K_{pilot}	Pilot Gain
T_{Lead}	Pilot Lead
T_{Lag}	Pilot Lag
τ	Pilot Intrinsic Delay
X_{pilot}	Pilot State
$p(t)$	Time Domain Pilot Elevator Command
$e(t)$	Time Domain Pitch Error
w_k	Process Noise
v_k	Measurement Noise
K_k	Kalman Gain
LOC	Loss Of Control
PIRAT	Pilot Research Aircraft
PVS	Pilot Vehicle System
UKF	Unscented Kalman Filter
WVU	West Virginia University

I. Introduction

Pilot is the most variable and difficult part of a Pilot-Vehicle System (PVS) to model and study.[1,2] It is important to develop pilot modeling tools which are simple to implement in real time but still gives necessary information to understand the pilot control behavior during conditions which affects the PVS stability. McRuer et al developed a simple transfer function model for compensatory pilot control.[3] Previous efforts in implementing and understanding McRuer pilot model has largely focused on batch estimation techniques[4–6] which uses data from a particular flight phase to estimate the average pilot model parameters. This is based on the assumption that pilot control parameters are reasonably constant during a flight phase. However it largely neglects situations (for example change in pilot behavior due to intrinsic factor such as stress, exhaustion etc.) where pilot model parameters might vary during a flight phase and could potentially

*PhD. Student, Mechanical and Aerospace Engineering (MAE) Department, PO Box 6106, tmandal@mix.wvu.edu, AIAA Student Member.
†Assistant Professor, MAE Department, PO Box 6106, yu.gu@mail.wvu.edu, AIAA Senior Member

make PVS unstable. Such variations in pilot model parameters might get hidden in the batch estimation analysis. This paper focuses on developing a real time estimation method based on Unscented Kalman Filter (UKF)[7] to estimate pilot parameters in real time and which will make it possible to track changes in the pilot model parameters as the flying condition changes. Since approach and landing is generally the most demanding phase of a normal flight it makes sense to study the human pilot control behavior closely during this phase.

Previous real-time pilot study involved wavelets[8] to estimate time-varying frequency response functions which is sensitive to measurement noise[9] and does not concern with estimating pilot model parameters. Other techniques include windowed maximum likelihood[9] estimator which can be slow in determining changing pilot parameters. The UKF on the other hand is easy to implement, relatively resistant to measurement noise and modeling error, and at the same time is a powerful estimator. Real time estimation of the pilot model parameters using McRuer pilot model is essentially a linear time varying system identification problem and UKF has been successfully used for such applications.[10–13] Even though McRuer pilot model is linear, the time domain equation used for estimation is non-linear in parameters to be estimated and UKF has been shown to perform well[14–16] for such non-linear problems. A recent use of UKF for studying manual control can be found in Ablamvi et al.[17] where it is used to monitor the human driver parameters in real time to identify situation when driver gets distracted. Another Kalman filtering technique used for human model parameter estimation is Extended Kalman Filter(EKF)[18,19] however it approximates a non-linear system with first order approximation and therefore may not be adequate for handling highly non-linear systems.

To properly validate UKF as a possible tool for human pilot study this paper uses data from both simulations and flight tests. It can be dangerous to carry out experiments such as time delay injection, actuator failure etc. during approach and landing phase of a flight in a manned aircraft. This makes sub-scale aircraft a valuable platform for getting real flight data to support and validate the pilot model parameter estimation algorithms. However, while flying sub-scale aircraft pilot lacks motion cues and only uses vision feedback to control the aircraft. This essentially reduces the system into a single input single output (elevator control) system which is then used to study human pilot compensatory control.The use of UKF to estimate pilot model parameters can provide insight into conditions when pilot behavior changes both abruptly and gradually. It can be used to monitor pilot in real time and study properties such as pilot's adaptation time and even predict when PVS becomes unstable. This paper explores the use UKF for human pilot compensatory control but can be extended to pursuit control or a combination of both type of control.

The rest of the paper is organized as follows. Section II presents a description of the sub-scale aircraft used to collect flight data and flight experiments carried out. Section III presents the formulation of equations which are used in UKF for pilot parameter estimation. Section IV presents simulation results and Section V presents results from flight tests. Finally Section VI contains discussion about the observations obtained and the conclusion.

II. PIRAT Test Bed

PIRAT (Pilot Research Aircraft) is an off-the-shelf (NitroPlanes TT-62 Alekto) remotely controlled sub-scale aircraft, which has been modified to carry out various experiments involving human pilot. Being a mass produced off-the-shelf platform PIRAT is inexpensive and easily replaceable which makes it ideal for riskier flight tests (such as actuator failure during landing) which might lead to loss of aircraft. PIRAT can be equipped with two different sizes of the wings and hence with different handling qualities. The following subsections provide a brief description of PIRAT's hardware and software.

II.A. Hardware

PIRAT is equipped with Gen-VI avionics developed at Interactive Robotics Laboratory at West Virginia University,Figure 1 shows the PIRAT research aircraft complete system and Table 1 provides detailed description of PIRAT characteristics. Gen-VI avionics consists of a Netburner® MOD54415 32-bit 250 MHz microcontroller module. It has 64 MB DDR2 RAM and 32 MB flash which enables the designer to run basic flight test algorithms (such as time delay injection in pilot command and actuator rate limiting) along with low level tasks such as recording sensor data and controlling servos for control surface actuation. Gen VI avionics also has an option to connect to a PC104 form factor computer to execute more computationally heavy processes. Gen-VI also consists of an Analog Devices® ADIS16485 Inertial Measurement Unit (IMU)

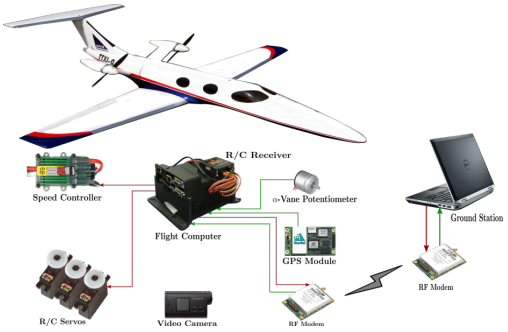

Figure 1: PIRAT aircraft and main avionics hardware.

Table 1: PIRAT Characteristics.

Property	**Value**
Wing Span	1.65 m, 2.03 m
Wing Area	0.39 m^2, 0.48 m^2
Fuselage Length	1.68 m
Flying Weight (With Payload)	6.80 Kg
Typical Speed	30 m/s
Power Plant	2 x Electric Brushless Motor

for measuring 3-axis accelerations and angular rates. A Specktrun® AR12120 R/C receiver sends pilot commands (received from transmitter) to MOD54415 via a serial-TTL connection. Gen-VI avionics can operate in manual, fully autonomous or Pilot-In-The-Loop (PIL) mode in which pilot command is modified by the Gen-VI depending on the state of a control switch (received along with other channels in MOD54415 from R/C receiver). Control switch is a physical switch on the R/C transmitter which always remains in pilot's control to change between different modes of flight (manual, automatic or PIL mode) and also for manual override during emergencies. All the flight data are saved on a microSD card installed in a slot conveniently mounted on the MOD54415 module.

In addition to the IMU PIRAT is also equipped with a Novatel® OEM615 GPS receiver,a Sakae® friction less analog potentiometer for angle of attack measurement, a Sony HDR-AS10 camera for recording flight video, and a Freewave® wireless modem to communicate with a simple ground station used by the experimenter. The ground station consists of another Freewave® wireless modem MM2 and a simple computer interface for the experimenter to add various amount of time delay and rate limit values or to change the center position of the aircraft elevator servo. The elevator control surface is actuated by a HiTec® HS-5245MG digital servo and its dynamics can by approximated by a 1st order transfer function given by

$$\frac{\delta_e}{\delta_c} = \frac{1}{0.076s + 1} \tag{1}$$

Where δ_e is the actual elevator deflection and δ_c is the commanded elevator deflection. The Eqn.1 was obtained by providing a step input to servo and recording the actual deflection using a potentiometer attached to the elevator. Also PIRAT elevator servo to pitch angle transfer function is given by

$$G(s) = \frac{-15.44s - 59.93}{s^3 + 3.59s^2 + 22.25s} \tag{2}$$

The PIRAT system transfer function is obtained using an earlier aircraft Parameter Identification (PID) flight experiments. The details of the procedure can be found in Gururajan et. al.[20]

A latency analysis was also carried out to find the delay between the instant pilot moves the control stick and the instant of actual movement of the control surface for PIL mode. The system latency for PIL mode for elevator control surface was found to be 40 ms.

II.B. Software

The software is written for MOD54415 and in C++ language. For obtaining estimates of the aircraft pitch angle the IMU and GPS data are post processed with a 9 state EKF.[21] For real time application the EKF can be implemented on a PC104 computer[22] connected to Netburner module in Gen-VI. As mentioned in Section II.A the pilot can use the control switch to change to PIL mode but what experiment is carried out (e.g.,time delay, rate limiting, or a combination of two) depends on the experimenter command using the ground station.This removes the pilot's ability to predict any failure mode and preempt it.Figure 2 shows the general flow of data and commands in the PIRAT software architecture.

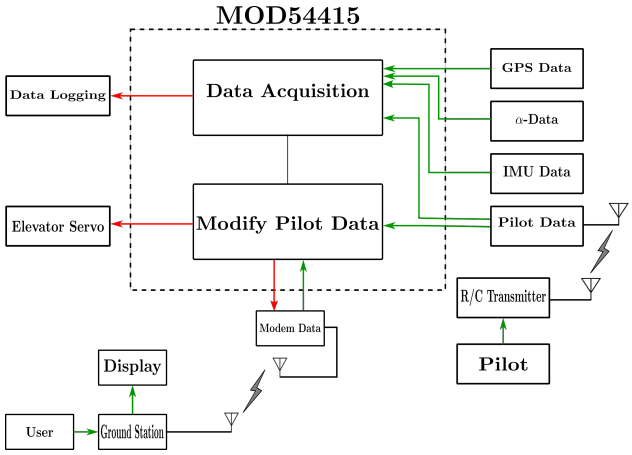

Figure 2: Data and command flow diagram in PIRAT.

II.C. Flight Experiments

As mentioned before,all human pilot studies on PIRAT were carried out for the approach and landing phase. During the flight test pilot was asked to carry out numerous touch and go (which involves trying to land on a runway and take off again without coming to a full stop). This adds extra workload on the pilot and is suitable for gaining insight into pilot control behavior during such strenuous flight conditions. Figure 3 shows flight data during a normal (no failure injection) touch and go flight experiment. It is possible to carry out multiple touch and go attempts during one flight with various failures injected from the ground station with no advance knowledge to the pilot. To reduce any inherent bias, the pilot was asked to land from each end of the runway and also to maintain consistency the pilot was asked to touch down within a particular area[23] of the runway. In Figure 3 it can be seen that pilot attempts four touch and go and as

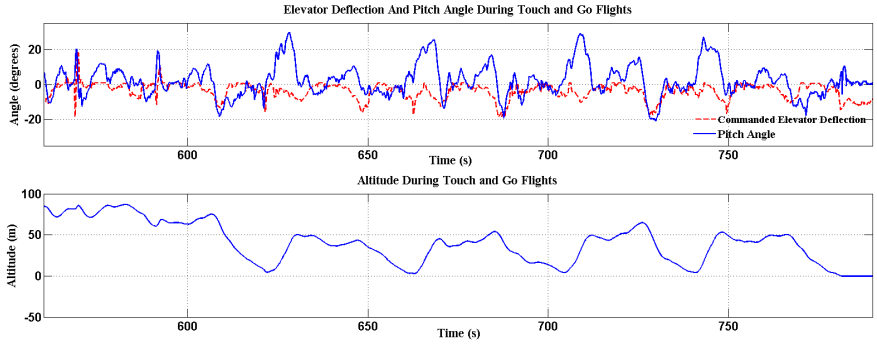

Figure 3: Flight Data during Touch and Go Experiment of PIRAT.

mentioned above pilot alternates between the end of the runway from which he/she attempts the landing.

III. Problem Formulation

This section provides a detailed description of the equations used for estimation purpose. The McRuer pilot model[3] is given by

$$P(s) = K_{pilot}\frac{T_{Lead}s+1}{T_{Lag}s+1}e^{-\tau s}E(s) \tag{3}$$

Where P(s) is frequency domain pilot command and E(s) is frequency domain pitch angle error, K_{pilot} is pilot gain, T_{Lead} is pilot lead, T_{Lag} is the pilot lag and τ is pilot intrinsic delay. The parameters that needs to be estimated are K_{pilot},T_{Lead},T_{Lag} and τ. Eqn.3 can be written in time domain as

$$\begin{aligned}\dot{X}_{pilot}(t) &= \frac{1}{T_{Lag}}X(t) + e(t-\tau)\\ p(t) &= \frac{K_{pilot}(T_{Lag}-T_{Lead})}{T_{Lag}^2}X_{pilot}(t) + \frac{K_{pilot}T_{Lead}}{T_{Lag}}e(t-\tau)\end{aligned} \tag{4}$$

In Eqn.4 $p(t)$ is time domain pilot output and $e(t-\tau)$ is the time domain pitch angle error delayed by τ seconds. $X_{pilot}(t)$ is 1×1 pilot state which needs to be solved for using the differential equation in Eqn.4 to calculate pilot output $p(t)$. The time delay is approximated by a first order Pade approximation(Eqn.5) to make the pilot model amenable to linear system analysis methods (e.g. bode analysis, state space expression etc.) and the new transfer function is given by Eqn.6.

$$e^{-\tau s} = \frac{2-\tau s}{2+\tau s} \tag{5}$$

$$P(s) = \frac{-\tau T_{Lead}K_{pilot}s^2 + (2T_{Lead}-\tau)K_{pilot}s + 2K_{pilot}}{\tau T_{Lag}s^2 + (2T_{Lag}+\tau)s + 2} \tag{6}$$

Converting Eqn.6 to controllable canonical state space form gives Eqn.7

$$\begin{aligned}\dot{X}_{pilot}(t) &= A_{pilot}X_{pilot}(t) + B_{pilot}e(t)\\ p(t) &= C_{pilot}X_{pilot}(t) + D_{pilot}e(t)\\ A_{pilot} &= \begin{bmatrix} \frac{-(2T_{Lag}+\tau)}{\tau T_{Lag}} & \frac{-2}{\tau T_{Lag}} \\ 1 & 0 \end{bmatrix}, B_{pilot} = \begin{bmatrix} 1 \\ 0 \end{bmatrix}\\ C_{pilot} &= \begin{bmatrix} \beta & \beta_2 \end{bmatrix}, D_{pilot} = b_0\\ b_0 &= \frac{-T_{Lead}K_{pilot}}{T_{Lag}}, b_1 = \frac{(2T_{Lead}-\tau)K_{pilot}}{\tau T_{Lag}}, b_2 = \frac{2K_{pilot}}{\tau T_{Lag}}\\ \beta_1 &= b_1 - Da_1, \beta_2 = b_2 - D*a_2\\ a_1 &= \frac{(2T_{Lag}+\tau)}{\tau T_{Lag}}, a_2 = \frac{2}{\tau T_{Lag}}\end{aligned} \tag{7}$$

Where $X_{pilot}(t)$ is 2×1 pilot state vector, A_{pilot} is the 2×2 pilot system matrix, B_{pilot} is the 2×1 pilot control matrix, C_{pilot} is the 1×2 pilot output matrix and D_{pilot} is the 1×1 pilot feed-forward matrix. Discretizing Eqn.7 gives the following

$$\begin{aligned}X_{pilot_k} &= A_{pilot_d}X_{pilot_{k-1}} + B_{pilot_d}e_{k-1}\\ A_{pilot_d} &= e^{A_{pilot}T_s}, B_{pilot_d} = A_{pilot}^{-1}(A_{pilot_d}-I)B_{pilot}, T_s = \text{Sampling time}\\ p_k &= C_{pilot}X_{pilot_k} + D_{pilot}e_{k-1}\end{aligned} \tag{8}$$

In Eqn.8 A_{pilot_d} is the 2×2 discretized pilot system matrix and B_{pilot_d} is the 2×1 discretized pilot control matrix. For both PIRAT system and the simulation carried out the sampling time T_s was set to 0.01 second and k is the time step at time kT_s and similarly $k-1$ is the time step at $(k-1)T_s$. It is evident from Eqn.7 that the equation is non-linear in parameters to be estimated.

III.A. Unscented Transformation and UKF

Unscented Transformation (UT) is used to handle non-linearity in $Y = f(X)$, where X and Y are $L \times 1$ vectors (here L is the length of the state vector), and f is an $L \times 1$ vector-valued function. Here, X is a random variable with mean, $\bar{X}$, and covariance,P_x. UT is central to UKF as it provides a statistical alternative to analytical linearization used in EKF. Great deal of work has been done on UKF for non-linear estimation problems and details can be found in existing literature.[24–26] For pilot parameter estimation problem it is assumed that the process and measurement noise terms are additive, as in

$$\begin{aligned} X_k &= f(X_{k-1}, e_{k-1}, p_{k-1}) + w_{k-1} \\ Y_k &= h(X_k, e_k, p_k) + v_k \end{aligned} \tag{9}$$

Where X is the state to be estimated and for the pilot estimation problem it is defined as $X = \begin{bmatrix} a_1, a_2, b_0, b_1, b_2, X_{pilot} \end{bmatrix}^T$. Also Y_k is the calculated pilot elevator command at time step k. The process and measurement noise are considered to be uncorrelated, white and Gaussian with zero mean and known covariance matrices Q and R respectively, as in

$$\begin{aligned} w_k &\sim N(0, Q_k) \\ v_k &\sim N(0, R_k) \\ E[w_k v_k^T] &= 0 \end{aligned} \tag{10}$$

Also in Eqn.9 f is the state propagation equation and h is the measurement equation given by

$$f = \begin{bmatrix} a_{1_{k-1}} \\ a_{2_{k-1}} \\ b_{0_{k-1}} \\ b_{1_{k-1}} \\ b_{2_{k-1}} \\ A_{pilot_d} X_{pilot_{k-1}} + B_{pilot_d} e_{k-1} \end{bmatrix}, h = \begin{bmatrix} C_{pilot} X_{pilot_k} + D_{pilot} e_k \end{bmatrix} \tag{11}$$

All the terms in Eqn.11 are derived in Eqn.7 and Eqn.8. At each time step k, a set of sigma-points are generated from the state estimate and covariance at time step $k-1$.[25] At each time step the state predicted using Eqn.9 is corrected or in other words updated using the actual pilot elevator command measured at that time step. The extent of correction is dependent on the Kalman Gain(K_k) calculated from UKF algorithm.[25]The update equation for X is given by

$$\hat{X}_k = \hat{X}_{k|k-1} + K_k(Y_k - \hat{Y}_{k|k-1}) \tag{12}$$

Where $Y_k = pilot_k$ is the actual pilot elevator command measured at time step k. In Eqn.12 $\hat{X}_k$ is the updated state at time step k, $\hat{X}_{k|k-1}$ is the predicted state at time step k from Eqn.9 and $\hat{Y}_{k|k-1}$ is the predicted output at time step k from Eqn.9. The parameters K_{pilot}, T_{Lead}, T_{Lead}, τ can then be obtained from the state X using the Eqn.7.

IV. Simulations

To validate the estimation algorithm a simulation was setup in Simulink® to generate flight data. This section provides a description of the simulation setup and results.

IV.A. Simulation Setup and Result

The simulation model consists of closed-loop PVS with unity feedback and pilot model in simulation is implemented in state space form provided in Eqn.8. For all simulations the values of K_{pilot},T_{Lead},T_{Lag} were varied gradually however the value of τ was kept constant. It is assumed that since pilot is focused during landing, the intrinsic delay does not vary significantly. The simulations were carried out for various values of τ and varying degree of changes in K_{pilot},T_{Lead},T_{Lag} parameters. Figure 4 shows the simulation scheme

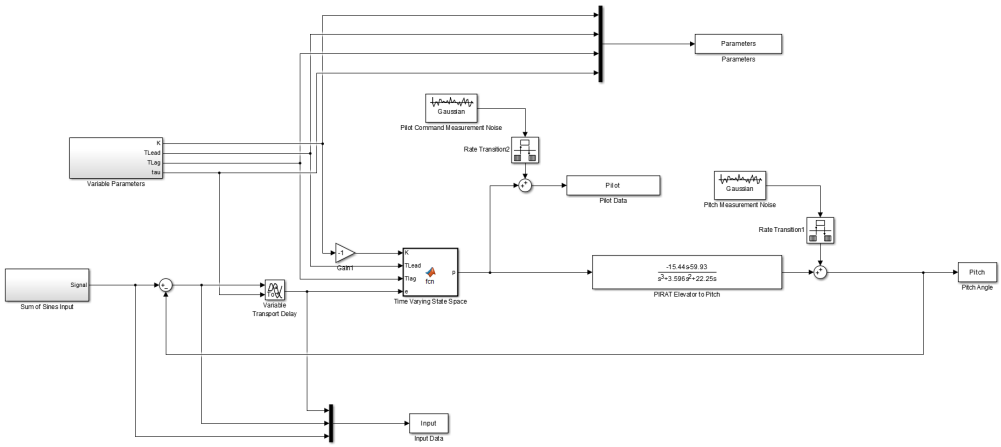

Figure 4: Simulation setup.

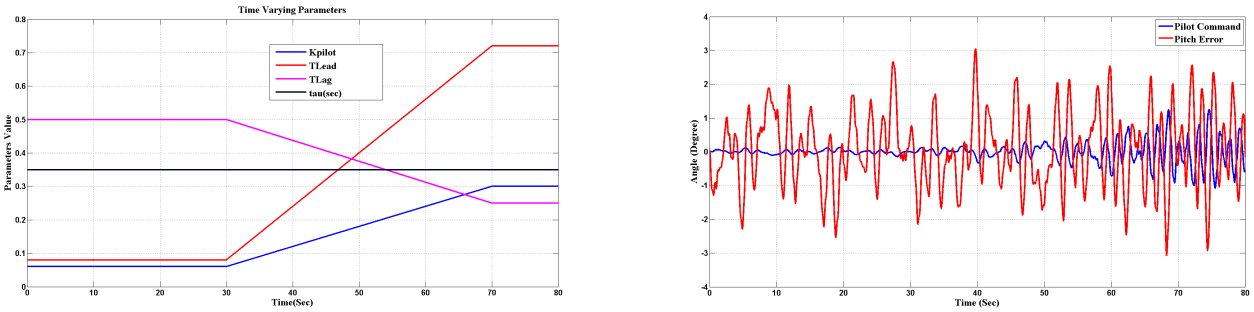

(a) Time varying parameters values.

(b) Pilot command and pitch error value.

Figure 5: Typical data generated by simulation.

developed to generate simulation data. The input i.e the reference pitch angle to the system is a sum of sines which covers the frequency range of human control (0.1-20 rad /s).[9] Figure 5 shows one example of varying parameters and measurement values used in a typical simulation. Figure 6 shows the estimation result obtained for the simulation data shown in Figure 5.

The result shows UKF has a good performance regarding tracking changes in the pilot model parameters under this particular simulation setup. However it is necessary to quantify the performance of the estimator under modeling error as human pilot being highly variable may not always behave like McRuer lead-lag pilot. To study the effect of modeling errors further simulations were carried out with pilot model different than McRuer lead-lag pilot model while using the UKF to estimate parameters for a McRuer lead-lag pilot model. To quantify the performance of UKF estimator the gain margin and phase margin of the PVS obtained using the estimated pilot model is compared with that of PVS using the true pilot model.Figure 7 shows the bode plot for true PVS and estimated PVS at 25 s, 60 s and 80 s. The true pilot model used is given by

$$P(s) = \frac{K_{pilot}}{T_{Lag}s + 1} e^{-\tau s} \tag{13}$$

In Eqn.13 the parameters K_{pilot},T_{Lag}, and τ are varied according to Figure 5a however parameter T_{Lead} is not used. It can be seen from Figure 7 that the bode plot for true PVS and estimated PVS at time step before the change in parameters, during the change in parameters, and after the change in parameters match very closely.Table 2 presents the gain and phase margin for true and estimated PVS. It is clear from Table 2 that the true PVS and estimated PVS has very similar stability characteristic i.e phase and gain margins. Similar results were also obtained for simulations carried out with $\frac{0.2K_{pilot}}{s}$ and $\frac{2K_{pilot}}{T_{Lag}s^2+s+1}$ as true pilot models.

The ability to predict the stability characteristics of the true PVS is of interest to predict Pilot Induced Oscillations (PIO). Simulation results show that UKF based pilot parameter estimation provides correct

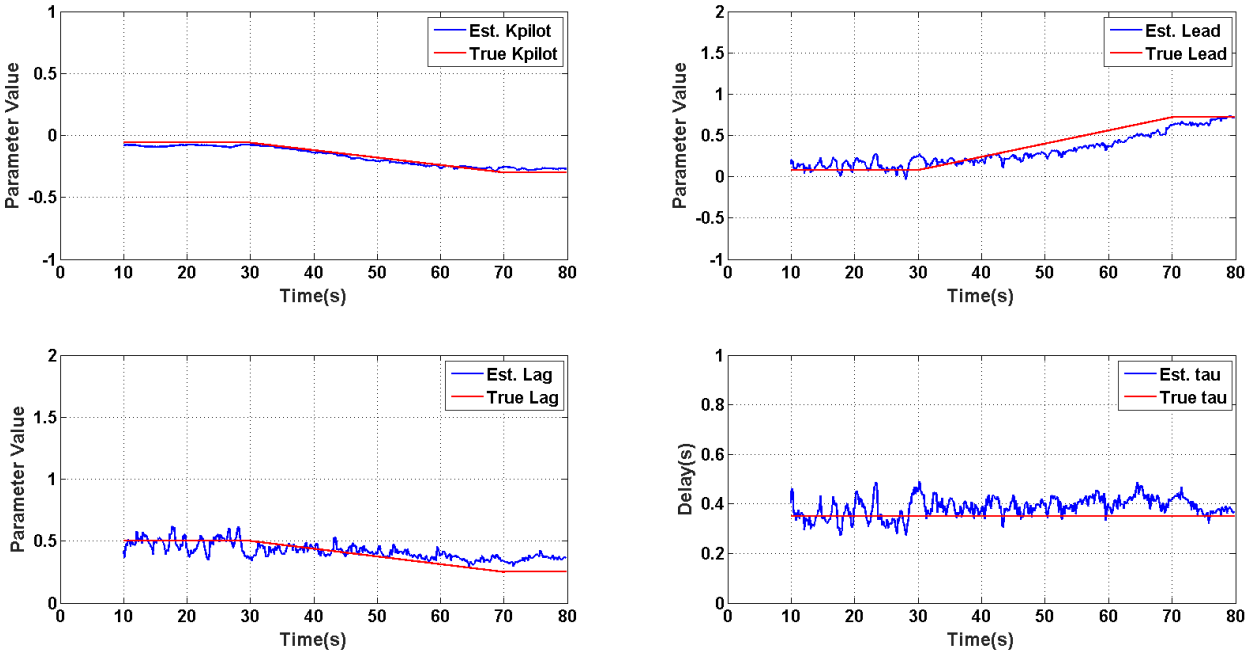

Figure 6: Pilot model parameter estimation results.

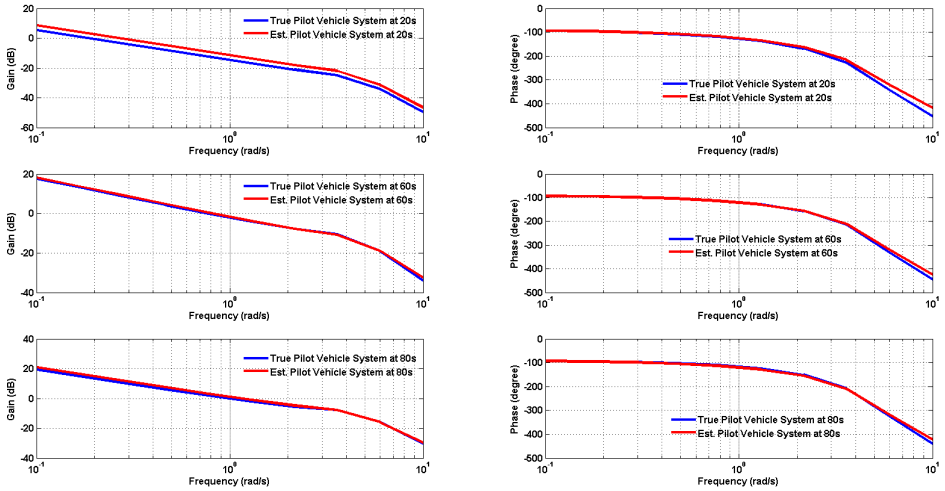

Figure 7: Bode plot of true and estimated PVS at different time.

stability characteristics of PVS even under substantial modeling errors.

V. Pilot Parameter Estimation from Flight Data

The UKF developed in Section III.A was also applied to actual flight data collected with the PIRAT sub-scale aircraft. The way flight experiments were conducted as described earlier in Section II.C) ensured that the pilot follow a consistent glide slope and pitch angle trajectory. Twenty four sets of touch and go data from PIRAT was used to calculate a mean pitch trajectory that pilot appeared to follow, which is later used as the reference pitch trajectory. Figure 9 shows the pitch trajectory during landing of seven different touch and go attempts and also the mean pitch trajectory. Figure 8 shows the glide slope during the landing of the same seven sets of touch and go flight experiment data and the mean glide slope. Only the part of the glide slope between the altitude of 30m and 9m was used as the pilot typically starts flaring up and slowing down after that during which the linear aircraft model developed for PIRAT becomes less accurate. The

Table 2: Stability margin comparison between true PVS and estimated PVS.

	True PVS	**Est. PVS**
At 20 s		
Gain Margin	22.1 dB at 2.46 rad/s	19.8 dB at 2.66 rad/s
Phase Margin	82.9° at 0.188 rad/s	80.3° at 0.275 rad/s
At 60 s		
Gain Margin	9.25 dB at 2.79 rad/s	9.48 dB at 2.85 rad/s
Phase Margin	67.6° at 0.769 rad/s	65.5° at 0.814 rad/s
At 80 s		
Gain Margin	6.97 dB at 2.94 rad/s	6.58 dB at 2.87 rad/s
Phase Margin	63.9° at 0.984 rad/s	55.6° at 1.15 rad/s

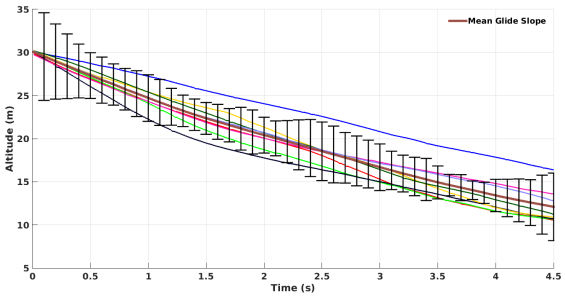

Figure 8: Glide slope during landing of touch and go experiments.

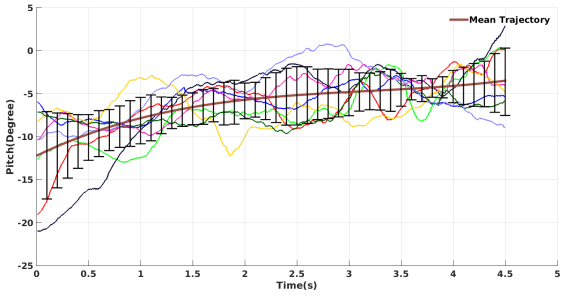

Figure 9: Pitch angle during landing of touch and go experiments.

vertical bars in both Figure 9 and Figure 8 shows the 1-σ deviation from the mean values.

V.A. UKF Result for Flight Data

A typical data set used for estimation of pilot parameter from flight data during a touch and go experiment is shown in Figure 10. It can be noticed that the typical time window for data set is ∼4 seconds therefore UKF

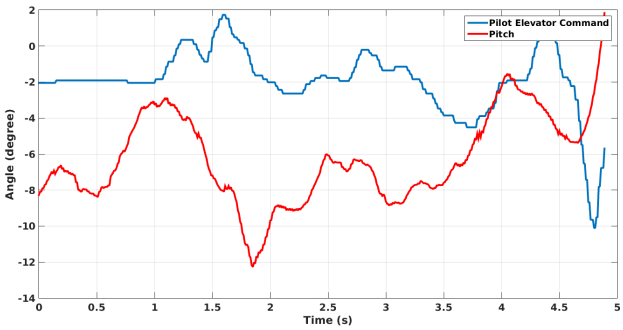

Figure 10: Typical landing data used for pilot parameter estimation.

should be designed and tuned properly to be able to converge in that time duration or. Other alternative is to start the UKF before the pilot starts the landing process, however in this paper only data during the landing process is considered to show the UKF is robust and converges fast. Figure 11 shows the estimation result

for five touch and go landing attempts during a single flight experiment. Similar analysis of landing attempts during other flights were also carried out. It was observed that the estimation is sensitive to initial value of

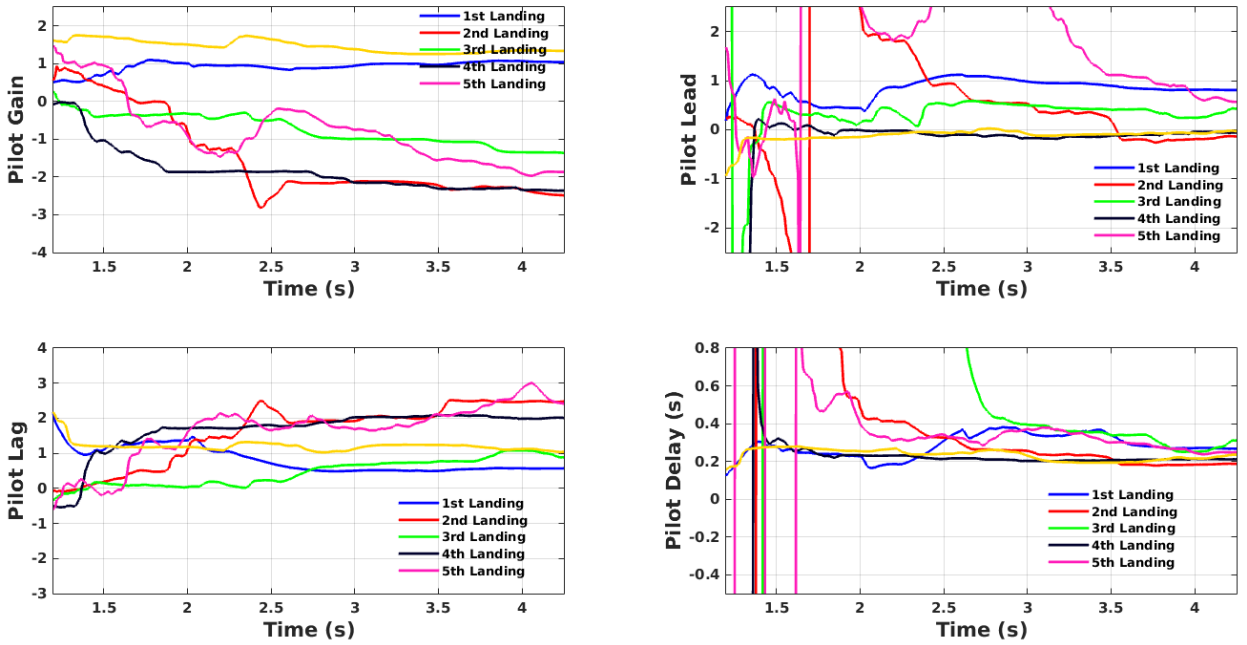

Figure 11: Pilot parameter estimated for real flight data.

state and the process noise covariance. An initial parameter value of $X = [3, 2.7, 4, 1, 0.8, 10, 2, 0.1, 0.1, 0.1]^T$ with small values of process and measurement noise provides fast convergence. For normal landing it was observed that the estimation converges at around 2.5 seconds for most flight data set. The pilot delay value for most landing is bounded between 0.2s-0.4s excluding the system delay of 0.04 s after the estimator converges.

Similar to the simulation study the estimated pilot model parameters were used to calculate the stability margin of the PVS. Table 3 provides the PVS stability margin calculated using estimated pilot model parameters at 4 s. It can be seen that estimated pilot model parameters at 4 s into approach during a touch

Table 3: Stability margin of the PVS estimated from real flight data.

	Gain Margin	**Phase Margin**
1st Landing	12 dB at 9.72 rad/s	93.8° at 5.94 rad/s
2nd Landing	-7.66 dB at 1.03 rad/s	-25.9° at 1.77 rad/s
3rd Landing	2.61 dB at 2.85 rad/s	16.8° at 2.12 rad/s
4th Landing	-4.9 dB at 1.48 rad/s	-16.6° at 1.96 rad/s
5th Landing	3.29 dB at 3.48 rad/s	34° at 1.89 rad/s

and go experiment predicts unstable system for second and fourth landings. However actual landings did not show any instabilities and the pilot also did not mention any difficulties in controlling the aircraft. A typical approach and landing lasts for ∼4 s and it can be assumed that pilot model parameter estimated at 4 s is not representative of the entire time period as the pilot model parameters are assumed to be time varying. Therefore it can be argued that pilot model parameters changes from unstable values before the PVS system diverges and pilot losses complete control. Other possible explanation for the mismatch in calculated PVS stability margin and observation in actual flight are, inaccurate aircraft model during flaring at the end of landing attempt,UKF converges to wrong set of parameters or not fully converged in short duration,a major portion of pilot output is contributed by non-linear remnant[27,28] or a major difference in the underlying

pilot model.

The UKF estimator would also gives incorrect results if the flight data does not have enough variations in it due to a lack of observability. Therefore further studies needs to be carried out to find a way to quantify estimator performance when applied to real flight data.

VI. Conclusions

This paper presents a UKF based technique for estimating McRuer pilot model parameters in real time. The estimator formulated in this paper was shown to be able to estimate true parameters with good accuracy in simulation studies.It was also shown that under modeling errors the estimator is still able to estimate parameters for a lead-lag pilot model such that the stability characteristics of the estimated PVS is similar to real PVS. The estimator was tested on real flight data collected with a sub-scale aircraft. It is difficult to verify the result of estimation result when applied to real flight data as true pilot parameters are not known. Therefore further studies need to be done to properly quantify the estimator performance when applied to real flight data. Additionally, more simulations needs to be carried out to analyze how non-linear remnant affects the estimator. It was also observed that the parameter at single point of time may not fully characterize the PVS stability. It might be necessary to consider how the stability of PVS is evolving with time due to parameters being estimated in real time and not remaining strictly constant.

The study in this paper was carried out with constant pilot delay assumption. In future studies this assumption can be relaxed. Also the current study only considers gradual changes in other pilot model parameter. Similar studies can be carried out for step change in pilot model parameter which may characterize Category 2 or 3 PIO.[29]

Currently work is being carried out at WVU to study the estimator prediction capabilities when different failures such as time delay and actuator rate limit is injected into the PVS. Such studies can help quantify estimator prediction capabilities if the estimator can correctly predict the stability of PVS after different failure injection in PVS or modify the estimator formulation based on such studies.

VII. Acknowledgments

This research was supported in part by NASA grant # NNX12AM56A.

References

[1]Young, L., "On adaptive manual control," *Ergonomics*, Vol. 12, No. 4, 1969, pp. 635–674.

[2]Kelley, C. R., "Manual and automatic control; a theory of manual control and its application to manual and to automatic systems," 1968.

[3]McRuer, D. T. and Krendel, E. S., "Mathematical models of human pilot behavior," Tech. rep., DTIC Document, 1974.

[4]Pool, D. M., Zaal, P. M., Damveld, H. J., van Paassen, M. M., and Mulder, M., "Pilot equalization in manual control of aircraft dynamics," *Systems, Man and Cybernetics, 2009. SMC 2009. IEEE International Conference on*, IEEE, 2009, pp. 2480–2485.

[5]Mandal, T. and Gu, Y., "Pilot-Vehicle System Modeling Using Sub-Scale Flight Experiments," *SciTech,AIAA*, 2013.

[6]T. Zaal, P. M., Pool, D. M., Chu, Q., Mulder, M., Van Paassen, M., and Mulder, J., "Modeling human multimodal perception and control using genetic maximum likelihood estimation," *Journal of Guidance, Control, and Dynamics*, Vol. 32, No. 4, 2009, pp. 1089–1099.

[7]Wan, E., Van Der Merwe, R., et al., "The unscented Kalman filter for nonlinear estimation," *Adaptive Systems for Signal Processing, Communications, and Control Symposium 2000. AS-SPCC. The IEEE 2000*, IEEE, 2000, pp. 153–158.

[8]Thompson, P. M., Klyde, D. H., and Brenner, M., "Wavelet-based time-varying human operator models," *AIAA Paper*, Vol. 4009, 2001, pp. 6–9.

[9]Zaal, P. M. and Sweet, B. T., "Estimation of time-varying pilot model parameters," *AIAA Modeling and Simulation Technologies Conference, Portland, OR (8–11 August 2011)*, 2011.

[10]Wu, M. and Smyth, A. W., "Application of the unscented Kalman filter for real-time nonlinear structural system identification," *Structural Control and Health Monitoring*, Vol. 14, No. 7, 2007, pp. 971–990.

[11]Chowdhary, G. and Jategaonkar, R., "Aerodynamic parameter estimation from flight data applying extended and unscented Kalman filter," *Aerospace science and technology*, Vol. 14, No. 2, 2010, pp. 106–117.

[12]Smyth, A., Masri, S., Chassiakos, A., and Caughey, T., "On-line parametric identification of MDOF nonlinear hysteretic systems," *Journal of Engineering Mechanics*, Vol. 125, No. 2, 1999, pp. 133–142.

[13]Crassidis, J. L. and Markley, F. L., "Unscented filtering for spacecraft attitude estimation," *Journal of guidance, control, and dynamics*, Vol. 26, No. 4, 2003, pp. 536–542.

[14]Xiong, K., Zhang, H., and Chan, C., "Performance evaluation of UKF-based nonlinear filtering," *Automatica*, Vol. 42, No. 2, 2006, pp. 261–270.

[15]Lefebvre, T., Bruyninckx, H., and De Schutter, J., "Kalman filters for non-linear systems: a comparison of performance," *International journal of Control*, Vol. 77, No. 7, 2004, pp. 639–653.

[16]Rhudy, M., Gu, Y., Gross, J., and Napolitano, M. R., "Evaluation of matrix square root operations for ukf within a uav gps/ins sensor fusion application," *International Journal of Navigation and Observation*, Vol. 2011, 2012.

[17]Ameyoe, A., Chevrel, P., Le-Carpentier, E., Mars, F., and Illy, H., "Identification of a Linear Parameter Varying Driver Model for the Detection of Distraction," *1st IFAC Workshop on Linear Parameter Varying systems*, 2015.

[18]Boer, E. R. and Kenyon, R. V., "Estimation of time-varying delay time in nonstationary linear systems: an approach to monitor human operator adaptation in manual tracking tasks," *Systems, Man and Cybernetics, Part A: Systems and Humans, IEEE Transactions on*, Vol. 28, No. 1, 1998, pp. 89–99.

[19]Schiess, J. R. and Roland, V. R., "Kalman filter estimation of human pilot-model parameters," 1975.

[20]Gururajan, S., McGrail, A., Gu, Y., Seanor, B., Napolitano, M., Prucz, J., and Phillips, K., "Identification of Aerodynamic Parameters for a Small UAV from Flight Data," *52nd Israel Annual Conference on Aerospace Sciences, Technion-IIT*.

[21]Gross, J. N., Gu, Y., Rhudy, M. B., Gururajan, S., and Napolitano, M. R., "Flight-test evaluation of sensor fusion algorithms for attitude estimation," *Aerospace and Electronic Systems, IEEE Transactions on*, Vol. 48, No. 3, 2012, pp. 2128–2139.

[22]Jarrell, J., Gu, Y., Seanor, B., and Napolitano, M., "Aircraft attitude, position, and velocity determination using sensor fusion," *AIAA Guidance, Navigation and Control Conference and Exhibit*, 2008, pp. 18–21.

[23]Brieger, O., Kerr, M., Leißling, D., Postlethwaite, I., Sofrony, J., and Turner, M., "Flight testing of a rate saturation compensation scheme on the ATTAS aircraft," *Aerospace Science and Technology*, Vol. 13, No. 2, 2009, pp. 92–104.

[24]Julier, S. J. and Uhlmann, J. K., "New extension of the Kalman filter to nonlinear systems," *AeroSense'97*, International Society for Optics and Photonics, 1997, pp. 182–193.

[25]Van Der Merwe, R., Wan, E. A., Julier, S., et al., "Sigma-point Kalman filters for nonlinear estimation and sensor-fusion: Applications to integrated navigation," *Proceedings of the AIAA Guidance, Navigation & Control Conference*, 2004, pp. 16–19.

[26]Rhudy, M., Gu, Y., and Napolitano, M. R., "An analytical approach for comparing linearization methods in EKF and UKF," *International Journal of Advanced Robotic Systems*, Vol. 10, No. 208, 2013.

[27]McRuer, D. T., Hofmann, L., Jex, H., Moore, G., and Phatak, A., "New approaches to human-pilot/vehicle dynamic analysis," Tech. rep., DTIC Document, 1968.

[28]McRuer, D. T. and Jex, H. R., "A review of quasi-linear pilot models," *Human Factors in Electronics, IEEE Transactions on*, , No. 3, 1967, pp. 231–249.

[29]Mandal, T., Gu, Y., Chao, H., and Rhudy, M., "Flight Data Analysis of Pilot-Induced-Oscillations of a Remotely Controlled Aircraft," *AIAA Guidance, Navigation, and Control Conference*, 2013.